ac Josephson Effect in Superfluid Helium†

B. M. Khorana*
Department of Physics, Case-Western Reserve University, Cleveland, Ohio, 44106
(Received 5 May 1969)

Two superfluid He baths were linked to each other through a small orifice. A quartz transducer produced a sound wave in the vicinity of the orifice, which served to couple the rate of vortex formation to the sound frequency. When the transducer was on, arrest of the flow at certain head differences was observed. The spacing between most of these steps in the flow curves was found to be in integral multiples of the basic unit $z_0 = h\nu/mg$, although in a few instances it was $(n_2/n_1)z_0$. A model for the phase slippage due to the motion of quantized vortex rings, which can account for the observed effect, is discussed. The stability of the liquid level at one of these "steps" appears to be indefinite: Once arrested, the liquid remains arrested until disturbed by fluctuations. These observations provide convincing confirmation of the ac Josephson Effect in liquid He II.

INTRODUCTION

Concepts derived from studies of superconductivity have stimulated advances in the understanding of superfluid He and vice versa. The experiments to be described in this paper are an outcome of this kind of cross fertilization.

London[1] was the first to recognize that the superfluids, superconductors and liquid He II, are systems exhibiting quantum properties on a macroscopic scale. Both these superfluids are found to show remarkable properties. Physically, the most dramatic manifestation of a superfluid is its ability to flow without any resistance. Mathematically, the basic property of a superfluid is the macroscopic occupation of a single quantum state, the "condensate". The condensate for liquid He is a consequence of the Bose-Einstein (BE) condensation phenomenon.[2-4] For the superconductors, this is a far more subtle matter. As a result, many years passed between the experimental discovery of superconductivity by Onnes[5] and the successful microscopic theory of Bardeen, Cooper, and Schrieffer.[6] The theory is based on the idea that in superconductors there is a net attraction between pairs of electrons of opposite spin and momentum $(\vec{p}\uparrow, -\vec{p}\downarrow)$. These bound pairs of electrons are known as Cooper pairs.[7] On the other hand, even though the nature of the condensate for liquid He has been understood[2] ever since 1938 a microscopic theory of liquid He, capable of explaining a variety of experimental results has not yet been formulated.

The state of macroscopic occupation is one of definite momentum, -zero, if the system is at rest. For a state of uniform flow, macroscopic occupation is that of the momentum state $\vec{p} = \vec{p}_S = m\vec{v}_S$, where v_S is the velocity of superfluid flow. The equilibrium density of superfluid mass flow is $\vec{j}_S \propto \vec{v}_S$, and the constant of proportionality is defined as the density ρ_S of the superfluid component. Therefore, $\vec{j}_S = \rho_S \vec{v}_S$.

Macroscopic occupation of a single quantum state has another important consequence, viz., it gives rise to long-range order in particle correlations.[3] It is this long-range order which produces the coherence phenomena in the superfluids.

To describe order-disorder transitions, one introduces a certain order parameter. This order parameter is taken to be different from zero in the ordered state and is zero in the disordered state. For example, in ferromagnetism, order parameter can be represented by spontaneous magnetization. For superfluids, macroscopic occupation of a single quantum state persists up to a certain critical temperature T_c, and therefore it is quite natural to define the order parameter by a quantity that characterizes the condensate. It can be defined as the mean value[8] of the destruction operator $\psi(\vec{r}, t)$, viz.,

$$\Psi = \langle \psi(\vec{r}, t) \rangle = f(\vec{r}, t)\, e^{i\gamma(\vec{r}, t)} ,$$

where this mean value is the average of ψ over a region, the extent of which is defined by appropriate coherence distances. For liquid He $\Psi(\vec{r}, t)$ is the wave function of the BE condensate. For superconductors, it is essentially the anomalous Green's function $F(\vec{r}_1, t_1; \vec{r}_2, t_2)$ introduced by Gor'kov[9] to describe the pairing of electrons. Because of the long-range order, the amplitude f, as well as, the phase γ have well-defined values over macroscopic regions of the superfluid. Thus, Ψ is truly a *complex* order parameter. f^2 gives the number of particles in the system, and γ describes current flow and external field effects.

The phase γ is a variable that is canonically conjugate to the particle number N, so that $\Delta N \Delta\gamma$

~ 1. The state of fixed N is an average over all values of phase, so that it is meaningless to talk about the phase of a superfluid sample as a whole. However, consider the case of two superfluid samples which are connected to each other through a barrier such that there is an overlap of wave functions of each other. The phase of the assembly as a whole is still not physical; but now there is a possibility of changes in the number density in the two samples due to the tunneling of particles back and forth through the barrier, and it becomes meaningful to talk about the relative phases of two such samples.

ac JOSEPHSON EFFECT IN SUPERCONDUCTORS

We have mentioned earlier that the phase γ of the complex order parameter is a variable which is canonically conjugate to the particle number N; so that γ may be regarded as the operator $i\partial/\partial N$. Therefore, $[\gamma, H] = -i\partial H/\partial N$, which together with the equation of motion $\dot{\gamma} = [\gamma, H]/i\hbar$ gives $\dot{\gamma} = \hbar^{-1}\partial H/\partial N$. Taking averages, this can be written in terms of the chemical potential $\mu \equiv \partial E/\partial N$,

$$\langle d\gamma/dt \rangle = \mu/\hbar \ . \tag{1}$$

This is called the Josephson frequency equation.[8,10]

If a chemical potential difference $\mu_1 - \mu_2$, is applied between two superfluid samples, Eq. (1) implies that the phase difference between the two changes by 2π during a time interval of $h/(\mu_1 - \mu_2)$. If the system has only one state for each value of γ, it should return to its original state when γ changes by 2π or an integral multiple thereof. Such arguments led Josephson[10] to conclude that there would be a periodic behavior, like ac superflow, across the barrier between the two superfluid samples at a frequency

$$\nu = (\mu_1 - \mu_2)/h. \tag{2}$$

For two superconductors having a voltage difference V across them, this characteristic frequency is

$$\nu = 2eV/h \ , \tag{3}$$

since this voltage implies a difference in chemical potential per electron pair of $2eV$. This corresponds to 1 $\mu V/483.6$ MHz. A direct observation of the ac Josephson supercurrent would be to look for the resulting high-frequency electromagnetic radiation in the vicinity of the junction of the two superconductors. The amount of power radiated by this supercurrent, as it turns out, is extremely small, though it has been detected by now.[11] However, the first experimental verification of ac Josephson effect came from indirect experiments, in which one beats the ac Josephson current against an externally applied microwave field. Two such experiments were done by Shapiro,[12] and Anderson and Dayem[13]: (i) Shapiro prepared a tunnel junction ($Al/Al_2O_3/Sn$) in the conventional way. He applied a microwave field at a fixed frequency ν_0 and measured the dc current-voltage characteristics of the junction. He observed "steps" where voltage is relatively constant for a considerable range of current, at values of voltage given by

$$V = n_2(h\nu_0/2e) \ .$$

(ii) Anderson and Dayem did a similar experiment in which the tunnel junction is replaced by a narrow thin-film superconducting bridge separating two superconductors. They observed steps along the voltage axis at voltages given by

$$V = (n_2/n_1)(h\nu_0/2e) \ , \tag{4}$$

where n_1 and n_2 are both integers. The phase slippage in this experiment was understood to be due to the motion of quantized flux lines in the vicinity of the connecting link, the thin-film bridge. This concept was explained by Anderson in more detail later.[8]

ac JOSEPHSON EFFECT IN SUPERFLUID HELIUM

Equation (2) can be equally well applied to the situation where the samples 1 and 2 are superfluid He baths instead of two superconductors. A difference z in head between the two baths gives a difference in chemical potential, so that the characteristic frequency of the ac superflow is

$$\nu = mgz/h \ , \tag{5}$$

which is the analog of Eq. (3). Here m is the mass of the He atom and g is the acceleration due to gravity. A frequency of 100 kHz corresponds to a step size $z_0 = 1.012$ mm.

Because of the heavier mass of the He atom, the tunneling medium in the case of superfluid He has to be correspondingly thinner than in the superconducting case (for the superconducting case, it is typically 20 Å). For quantum-mechanical tunneling, the barrier would have to be of subatomic dimensions. This presents a formidable experimental problem, and an analog of Shapiro's experiment has not been tried as yet. The next best experiment is an analog of the experiment of Anderson and Dayem, viz., one uses an orifice connecting the two superfluid baths, the orifice acting as the weak link analogous to the short thin-superconducting-film bridge. It was such a geometry that was tried by Richards and Anderson,[14] and they observed an indication

of this effect. The equivalent of the microwave field was provided by an ultrasonic transducer producing sound waves in the vicinity of the orifice. They noticed that the flow through the orifice, which separated the two superfluid baths, showed irregular behavior whenever the relation

$$n_1 mgz = n_2 h\nu \quad (n_1 \text{ and } n_2 \text{ integers}) \tag{6}$$

was satisfied.

Anderson's[8] concepts that motivated this experiment were extremely subtle. Important features were: (a) There should be arrest of fluid flow when relation (5) or (6) is satisfied. (b) Stability in these steps should be almost indefinite, only internal fluctuations can cause the liquid level to jump out of the arrested level.

No attempt had been made in Richards and Anderson's experiment to emphasize these aspects; so that we felt that enough justice had not been done to Anderson's ideas which are very basic and fundamental to a unified description of the two superfluids. Therefore, we considered it worthwhile to improve upon their experiment in order to exhibit this effect with convincing clarity.[15]

EXPERIMENTAL DETAILS

The main feature of the cryostat was a double-chamber arrangement, consisting of an outer chamber (OC) and the experimental or inner chamber (IC). A schematic diagram of the IC and OC together with a few other crucial parts is shown in Fig. 1. The actual experiment was carried out inside IC, which formed a completely closed chamber; although, when necessary, it could be connected to OC through a mechanical valve at room temperature.

OC was in fact the He Dewar of inside diameter 100 mm and IC was a 62-mm-diam copper-glass seal. IC was connected to the top flange by a 25-mm-diam stainless-steel tubing of thin wall. The helium liquid could be transferred to IC directly from a storage Dewar, as was done for

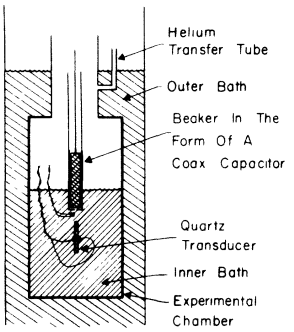

FIG. 1. Schematic of the low-temperature end of the apparatus.

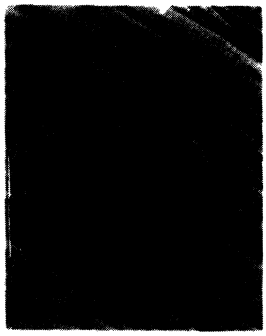

FIG. 2. Photograph of orifice in nickel foil.

OC also. The outer bath could be pumped with the aid of a large mechanical pump (Kinney pump, capacity 22 l/sec). As the temperature of the outer bath would decrease, the inner bath would also cool down since the IC and the OC were always in good thermal contact with each other.

This double-chamber arrangement (i) ensured that the level of the inner bath did not change perceptibly in the course of an entire run lasting several hours. This is important because we, after all, want to make measurements of height with respect to the inner-bath level and we would like to have the least amount of fluctuations in that; and (ii) provided a very stable thermal environment for the experimental chamber.

Thus, it eliminated the necessity of using the second beaker which Richards and Anderson were forced to incorporate in their experiment.

Beaker and Liquid-Level Measuring Probe

The construction of the beaker was such that it incorporated within itself the liquid-level sensing device. The beaker was in the form of a coaxial capacitor (Fig. 1) consisting of a solid cylindrical rod mounted coaxially inside a hollow cylindrical thin-walled tube and kept in position by 0.075-mm-thick Mylar spacers. To the top of the beaker was soldered a home-made coaxial line. This consisted of a 10-mm stainless-steel tubing with a copper wire (Gauge #26) stretched along its axis. The wire was kept in position by Teflon washers placed at suitable intervals along the length of the tubing. The coaxial line ended in a hermetically sealed BNC connector at the room-temperature end. The capacitance cell (i.e., beaker) could be raised or lowered from the outside by raising or lowering the 10-mm coaxial line, which passed through an o-ring seal at the top flange.

The bottom of the beaker was formed of a 4×10^{-3} cm-thick nickel foil which had an orifice of $\simeq 10^{-3}$ cm diam in it. A photograph of the orifice taken through a metallograph at approximately 1000× is reproduced in Fig. 2. The orifice is the dark area at the center of the photograph.

To ensure that the vapor pressure inside the beaker and outside it were the same, a few openings in the stainless-steel tubing of the coaxial line were made. These openings were made sufficiently high up that the temperature in their vicinity was much higher than 2.2 K. The superfluid film was thus made static before it reached these openings so that the orifice at the bottom of the beaker provided the only link through the liquid phase, between the volume of He II inside the beaker and that around it.

As the liquid flowed through the orifice, the height of the liquid in the annular space of the coaxial capacitance cell would change, thus causing a change in its capacitance. This is so because the dielectric constants of He vapor and liquid differ by about 5.5%. A depth gauge based on this principle was first used in liquid He by Boorse and Dash.[16]

To record the liquid flow through the orifice, the capacitance of this coaxial capacitor was monitored in time by using a capacitance bridge (General Radio, 1615A), a lock-in amplifier (Princeton Applied Research, JB-5) and a strip-chart recorder in sequence. To minimize the effect of fluctuations in the line voltage, ac power was fed to them through a sola transformer.

Ultrasonic Transducer

Frequency-control quartz crystals of fundamental frequency 100 and 150 kHz were used as transducers. The crystal was suspended from the bottom of the beaker and positioned in such a way that it was almost directly under the orifice in the nickel foil, and also as close to it as possible without actually touching it (Fig. 1). The two leads to the crystal faces were fed by an external oscillator (Hewlett-Packard Test Oscillator, 651A) through a transformer. The transformer was used to match the impedance of the oscillator to that of the crystal. The exact resonance of the crystal was detected by putting a suitable resistor R in series with the crystal and looking for a maximum in the voltage V_R across it as the oscillator was being tuned. The exact frequency at resonance was noted by connecting an electronic counter (Hewlett-Packard, 5244L).

Thermometry

The temperature was monitored by means of a $\frac{1}{10}$-W Allen-Bradley resistor, mounted in the vicinity of the orifice. Its resistance was measured with an ac Wheatstone bridge. The Wheatstone bridge and the temperature regulator were built according to the design of Blake and Chase.[17] In this arrangement, the off-balance voltage from the bridge is fed into a phase-sensitive detector which controls the dc current into a heater. The heater in our case was placed at the bottom of the outer bath. The desired temperature was set by dialing the corresponding resistance value on the bridge. When temperature increased from this value, the heater current was reduced; while a decrease in the temperature caused an appropriate increase in the heater current. In addition, a Cartesian manostat and a diaphragm-type manostate after Walker[18] were also incorporated in the pumping lines. By a suitable combination of these three temperature regulators, the temperature of the outer bath could be controlled both above and below the λ point. The experimental chamber was kept immersed in this constant temperature well-regulated bath. The outer bath also acted as a shield for the inner bath from the stray heat input, if any, from the outside.

An absolute pressure gauge (Wallace-Tiernan Gauge, 0–20 mm) was connected to IC, and was used for measuring the temperature of IC.

Preparation and Procedure for a Run

Special care was taken to keep the atmosphere inside IC and OC as clean as possible. The preparation for a run involved the following main steps: (i) While IC and OC were still at room temperature, they were both pumped hard for 3–4 days continuously. (ii) IC and OC were isolated from the pump, and He gas at slight overpressure (about 1 lb/in.^{2} above atmosphere) was introduced, and liquid N_2 was transferred into the N_2 Dewar. (iii) After the inside of IC had reached N_2 temperature, IC was isolated from OC. (iv) Liquid He was then transferred into OC. (v) OC was isolated from the outside atmosphere. (vi) The valve which connects IC with OC was slowly opened so that they reached pressure equilibrium with each other. In so doing, only the pure He gas obtained from the evaporation of the liquid in OC, was let into IC, thus maintaining the clean atmosphere of IC. (vii) After IC and OC had reached equilibrium, He liquid was transferred into IC.

IC was sealed off from the outside atmosphere and OC, and pumping on OC was started. Extreme care was taken in pumping to avoid extraneous vorticity being generated in either of the two baths. With this end in view, the pumpdown was done extremely slowly especially when going through the λ point. Above the λ point, there is a lot of bubbling of the liquid which causes its turbulent stirring. This gives rise to a large amount of vorticity in the liquid. The use of the double-chamber arrangement, where the experimental chamber was not at all pumped, provided an added advantage from this point of view. Most of the runs were made at 1.1–1.3 K, which once attained was regulated by the electronic regulator in conjunction with a manostat. In this way a temperature stability of better than $\pm$ 50 μK over

a period of 3–4 h could be attained. Of course, the short-term stability was much better than this. Once a thermally stable He bath was obtained, flow measurements were begun.

EXPERIMENTAL RESULTS

Before the nickel foil with the small orifice in it was soldered on to the bottom of the beaker assembly, a run was made in liquid He II. The capacitance of the beaker was measured for various heights of the liquid level inside it. The height was measured with the help of a cathetometer. In this way, the linearity of the annular region in the beaker was ascertained. This also gave us a calibration of the capacitance cell (beaker); 1 mm height of liquid in its annular space corresponded to a change in capacitance of 0.11 pF. However, the calibration was checked in the course of each run.

Gravitational Flow

It has already been mentioned that the beaker could be raised or lowered, with respect to the inner bath, from the outside. This provided the means of creating a head difference between the liquid inside the beaker and that around it. Once a head difference is created, the liquid would tend to equalize the levels. Such an inflow through the orifice is shown in Fig. 3. This is a reproduction of the recorder tracing of the capacitance (liquid level) against time. The horizontal part of the curve corresponds to equalized levels, while the sloping part of the curve corresponds to the flow of liquid. The curve represents a flow over a height of approximately 7 mm of the beaker, with a critical velocity of $\simeq 28$ cm/sec. This compares quite well with the observations of Richards and Anderson.[14] The general features of the outflow curves were found to be similar to those of the inflow curves, both showed a weak dependence on the pressure head. The essential feature to note is that these gravitational flow curves are smooth curves, which incidentally also shows that there are no irregularities present in the annular region of the beaker. In order to emphasize this point, we expanded the scale along the time axis by increasing the drive speed of the motor in the strip-chart recorded from 8 in./h to 8 in./min.; yet the flow curves did not show up any perceptible irregularities in the beaker.

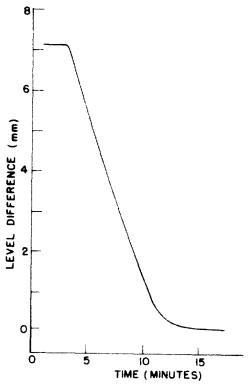

FIG. 3. Gravitational flow of liquid He II into the beaker. $T = 1.34$ K. The flow occurred over the same region of the beaker as in Fig. 5.

Effect of Sound Field on Fluid Flow

Once the liquid levels inside the beaker and outside it had equalized, the transducer was switched on, as at arrow marked A in Fig. 4(a) (power input into transducer $\simeq 225$ μW). The recorder trace shows that soon after the sound was switched on, liquid began to be pulled out of the beaker and that this outflow curve is not anywhere as smooth as that of gravitational flow in Fig. 3, rather, it has kinks on it at some head differences. The frequency of the transducer used was 99.722 ± 0.001 kHz and this corresponds to the Josephson step size $z_0 = 1.01$ mm which is appropriately indicated on the recorder tracing. The total difference in height created by this pumping action of the transducer is $\simeq 15$ mm in about 90 min. Almost all of the kinks, etc., on this curve could be related to spacings of either z_0 or $\frac{1}{2}z_0$. This was our first successful attempt at observing anything like what Richards and Anderson had reported. However, in order to identify these kinks as actual steps where arrest of liquid flow takes place, we looked into the various parameters that would help us in this objective. The power input into the transducer was obviously an important parameter as far as the rate of pumping and hence, the slope of the pumping curve was concerned. Figures 4 and 5 show the effect of decreasing the power input into the transducer. The pumping curves in Figs. 4(c) and 5 correspond to a power input of approximately 60 μW, the lowest power used in this series of runs. As the power is decreased, the steps begin to look well defined and the stability in these steps also increases – the liquid level stayed in one of these levels for as long as 25 min in Fig. 4(b) and for 40 min in Fig. 4(c).

In Fig. 5, one can see the steps at z_0, $2z_0$, $3z_0(?)$, $4z_0$, $5z_0$, and $8z_0$, the first few rather strikingly well. Figure 3 was in fact the gravitational flow, in the absence of sound, over the same region of the beaker as in Fig. 5 and at the same temperature. A comparison of these two figures shows the genuine nature of these steps very convincingly.

Figure 6 shows pumping curves with a transducer of frequency 149.815 ± 0.001 kHz corresponding to the basic step size $z_0 = 1.51$ mm. Figure 6 is slightly different in that sound has been superposed on a gravitational inflow curve. The general features of the previous pumping curves are borne out quite well (see Table I). There is clearly a preponderance of the steps of the kind $n_2/n_1 = 1$ at both transducer frequencies.

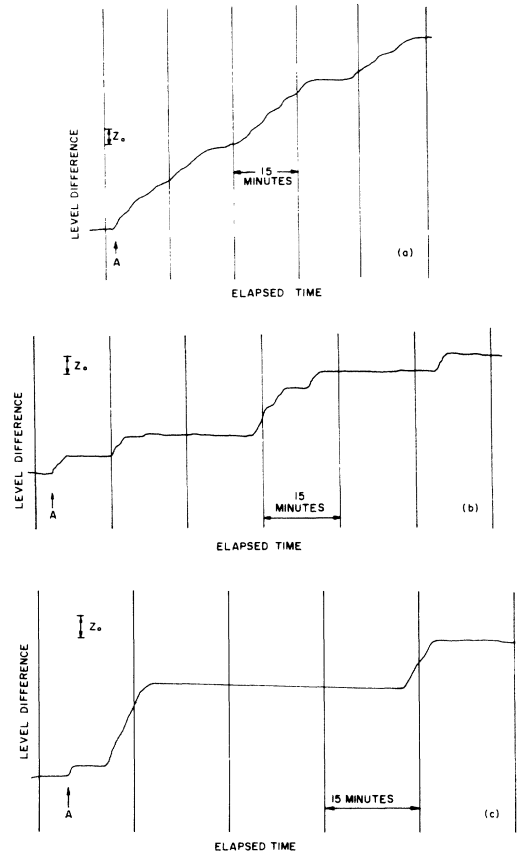

FIG. 4. Liquid-He head versus time due to the pumping action of transducer of frequency $\simeq 100$ kHz. The computed $z_0 = h\nu/mg = 1.01$ mm is indicated. In (a), power input $\simeq 225$ μW, $T = 1.28$ K; (b), power input $\simeq 100$ μW, $T = 1.25$ K; and (c), power input $\simeq 60$ μW, $T = 1.12$ K.

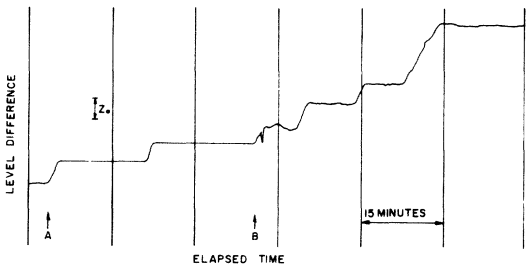

FIG. 5. Liquid-He head versus time due to the pumping action of transducer, at $T = 1.34$ K. The sound was switched on at point A, and the intensity was momentarily increased at point B in order to "kick" the level out of the step $2z_0$. The transducer was excited at 99.722 kHz with a power input of $\simeq 60$ μW. The computed $z_0 = h\nu/mg = 1.01$ mm.

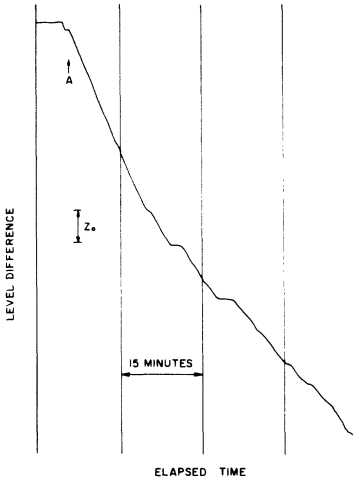

FIG. 6. Pumping action of the transducer superposed on gravitational flow into beaker. Transducer frequency $\simeq 150$ kHz, power input $\simeq 20$ μW, $T = 1.12$ K.

TABLE I. Total number of steps of the kinds $n_2/n_1 = 1, \frac{1}{2}, 2$ [refer Eq. (6)] observed at these two frequencies.

Transducer frequency	n_2/n_1 = 1	$\frac{1}{2}$	2
100 kHz	24	4	4
150 kHz	13	7	3

Stability of Liquid in the 'Arrested' Levels

Very often, when the liquid level appeared to have been arrested at one of these steps, it could be kicked out of the step by momentarily increasing the power input into the transducer. For example, in Fig. 5, initially the power input into the transducer was $\simeq 60$ μW at A. At the arrow marked B, the power was raised to $\simeq 500$ μW for a few seconds and quickly brought back to the original level of $\simeq 60$ μW. This technique was successful in kicking the liquid out of the "arrested" level a number of times. But for the success of this technique, we might never have been able to observe the steps beyond $2z_0$ in Fig. 5.

Figure 7 shows the effect of a *gradual* change in the power input into the transducer. The values of the voltages across the transducer in the course of that tracing of well over 3 h are marked. Two observations will suffice: (i) At some of the arrested liquid levels, an increase in the power input of as much as 100% was necessary to force the liquid out of that level, and (ii) the power input necessary to sustain the liquid at one of these steps was usually much lower than that required to pump to that level. This is exhibited in the uppermost step in this figure, where a decrease

in the power input from $\simeq 110$ to $\simeq 30$ μW did not drive the liquid out of that step.

DISCUSSION

We have been able to observe the complete arrest of the flow of liquid He at discrete head levels satisfying the Josephson frequency condition $n_1 mgz = n_2 h\nu$. The stability of the liquid at one of these steps appears to be indefinite – once arrested, the liquid remains arrested until disturbed by fluctuations. These fluctuations could be internal or external. The important features in our experiment that might have been responsible for the clarity with which we were able to observe the steps and their almost indefinite stability, were: (i) thermal stability of the experimental bath of liquid He, (ii) constant level of the inner bath, and (iii) slow pumpdown to the lowest temperature.

The steps have been observed up to a temperature of 1.76 K (Fig. 8), although they begin to fade away as the temperature is raised. The pumping action is, however, observed even above the λ point (Fig. 8).

Role of Transducer

The quartz transducer appears to have a dual role, that of inducing flow through the orifice, which has been referred to as the pumping action, and that of synchronization of phase variation.

(i) *Pumping action.* Whenever the transducer was turned on, the liquid began to be pulled out of the beaker into the bath in which the transducer was oscillating. Because of the closeness of transducer to the bottom of the beaker, the liquid in the gap between the transducer and the bottom of the beaker gets pushed in and out of this gap in a direction transverse to the axis of the orifice. This transverse velocity of the liquid is expected to generate vortices in the vicinity of the orifice and also cause a decrease in the pressure there resulting in the pulling of the liquid out of the beaker by virtue of the Bernoulli effect. We might

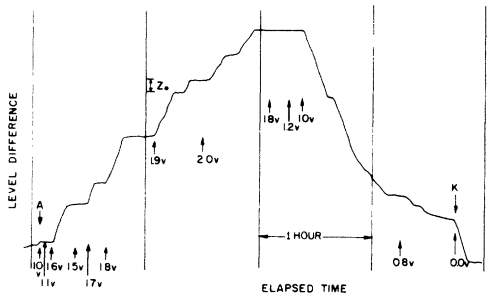

FIG. 7. Effect of gradual change in power input to transducer on stability of "arrested" levels. $\nu \simeq 100$ kHz, power input 0–110 μW, $T = 1.19$ K.

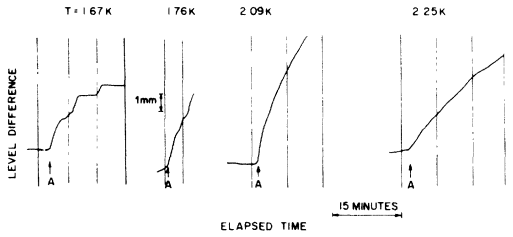

FIG. 8. Pumping action of transducer at different temperatures. Transducer switched on at point A. Steps can be identified up to $T = 1.76$ K. Pumping action is, however, observed even above the λ point.

note, in addition, that since the velocity v enters in the Bernoulli equation as its square, the direction of the transverse velocity is immaterial as far as the direction of the pumping action is concerned. The pumping action is observed in liquid He I also. Vorticity is, however, not quantized in He I.

The fountain effect will contribute to this pumping in liquid He II, because of the power dissipated by the transducer as heat. When an equivalent dc power was dissipated in a resistor in the vicinity of the orifice, the corresponding head produced could be barely detected. A dc power input of 1.0 mW in the vicinity of the orifice produced a fountain head of $\simeq 0.17$ mm at a temperature of 1.12 K This can be compared with the typical power input of 60 μW used in obtaining the curves of Fig. 4(c) and Fig. 5.

(ii) *Synchronization of phase variation.* We have already mentioned that there is a possibility for the generation of vortices near the orifice and their being carried across it by the transverse velocity of the fluid. Since there is a phase change of 2π in going around a vortex, one can expect a phase variation to be set up in this manner. The rate at which the vortices will be carried across the hole will have to be related to the frequency of the transducer in some way, in general, n_2 vortices in n_1 cycles of the transducer. This would correspond to a phase slippage at the rate of

$$\nu = (n_1/n_2)(mgz/h) \ .$$

A possible mechanism of this vortex generation and the phase slippage is as follows: When the liquid flows out of the orifice, vortex rings may be generated along the downstream according to Feynman's[19] picture. These rings have a polarity as shown in Fig. 9.

By having a transducer oscillating at a fixed frequency in the vicinity of the orifice, the tendency to form vortices will be increased in one half-cycle and decreased in the other half-cycle. This was, at least qualitatively, borne out by the observation that the velocity of the flow of liquid

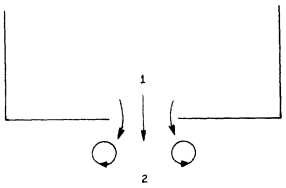

FIG. 9. Feynman's picture of vortex ring generation at the orifice linking two superfluid samples 1 and 2.

through the orifice when the transducer was on, was in fact less than the critical velocity of gravitational flow. Therefore, the vortex ring is presumably created more favorably during the contracting half-cycle of the transducer. This ring once formed is driven either to the left or to the right, away from the orifice. This drift velocity is provided by the net transverse velocity due to the asymmetry of the transducer with respect to the orifice. The motion of the ring across the orifice gives rise to the phase slippage.

In order to account for the observed direction of the pumping action, we need just to notice that a vortex of polarity like the one on the left in Fig. 9, moving from left to right gives an increase in the rate of phase change of bath 2 with respect to bath 1. Of course, it is obvious that the direction of pumping is unaffected whether the ring moves to the left or to the right.

Harmonic and Fractional Harmonic Steps

The observation of steps which are integral n_2 or fractional n_2/n_1 multiples of the basic step size $z_0 = (h\nu/mg)$, can be interpreted either due to the motion of n_2 vortices in n_1 cycles or due to the frequency modulation of the ac Josephson superflow. The former has already been discussed above. We will now discuss the latter. Across the orifice, there is (a) bias corresponding to the height difference z and (b) small ac bias, induced by the ultrasonic transducer, that oscillates at the frequency ν_0 of this transducer. Since the frequency of the Josephson superflow, ν_S, depends on the bias z, this has a small periodic variation in time due to the modulation frequency ν_0, i.e., the superflow is frequency modulated. Because of this, it contains components that have many frequencies. For an unmodulated wave,

$$z = z_1 \sin\nu_s t,$$

and for the frequency-modulated wave,

$$z = z_1 \sin[\nu_s (1 + m \sin\nu_0 t)t]$$

$$\equiv z_1 \sin[\nu_s t + m' \sin\nu_0 t]. \qquad (7)$$

Expanding this, one finds components having frequencies

$$\nu_s, \nu_s \pm \nu_0, \nu_s \pm 2\nu_0, \cdots$$

For one of these components,

$$\nu_s - n_2\nu_0 = 0, \quad \text{or} \quad \nu_s = n_2\nu_0, \qquad (8)$$

where n_2 is an integer and $\nu_S = mgz/h$. Therefore, at certain level differences, there is a dc superflow due to the beating of the superflow against some harmonic of the applied frequency. In a z-versus-t plot, this would correspond to a change in the slope at that level difference. If the magnitude and sign of this dc superflow are right, it is possible to have zero-slope regions in such a plot. The level differences at which these zero-slope regions occur are given by Eq. (8), viz.,

$$z = n_2(h\nu_0/mg) .$$

Only the harmonics of the fundamental step $h\nu_0/mg$, are expected if the coupling of the ac source to the bath is harmonic. However, if this coupling is anharmonic, one would expect Eq. (7) to contain higher-order terms as well, thus giving rise to components of all frequencies

$$n_1\nu_s \pm n_2\nu_0 ,$$

where n_1 and n_2 are integers. Thus, in general, the steps would occur at values of z given by

$$z = (n_2/n_1)(h\nu_0/mg) .$$

Other Possible Explanations of the Observed Effect

A possible source, other than the ac Josephson effect, for the appearance of the observed steps was considered by Richards and Anderson[14]; viz., a series of ultrasonic standing-wave resonances associated with the changing level of the liquid inside the beaker. They pointed out that in such a case, the step size (= half a wavelength) between such resonances would depend on the absolute head of He in the beaker and be inversely proportional to the frequency of ultrasonics. Besides these properties, which are different from those of the Josephson steps, we might add that there is approximately an 18% difference in the size of the two kinds of steps, in one case it is $\frac{1}{2}\lambda$; in the other $h\nu/mg$. The uncertainty in our measurement of the step size was never more than 10%.[20] This clearly permitted us to distinguish between the two possibilities. Besides, we do not observe any steps in liquid He I, thus providing another reason against the source of the steps to be these standing waves. In this manner, we were able to show beyond any doubt that the source

of the steps was not the ultrasonic standing-wave resonances. In any case, it would be more difficult to explain the fractional harmonic steps (of the kind $\frac{1}{2}z_0$) on the basis of the standing-wave phenomena.

It is possible[21] to get the result $mgz = h\nu$ from the concepts of perfect fluid hydrodynamics and quantization and conservation of vorticity. Anderson, himself, has then pointed out that the concept of vorticity quantization is not exact in the sense that it is based on the hypothesis that $\vec{v}_s = (\hbar/m)\nabla\gamma$ is the real particle velocity of the superfluid, according to him, this *can not* be proved. In fact, the much more fundamental and basic equation is the Josephson frequency equation (1)

$$\hbar(d\gamma/dt) = \mu \ .$$

Further, superfluidity is much more than perfect hydrodynamical flow. Sure enough, superflow on a macroscopic scale can be identified with perfect hydrodynamical flow as illustrated by the success of the quantum hydrodynamics introduced by Landau.[22] However, superfluidity is much more subtle; it involves long-range order. A real understanding must, therefore, be based on a microscopic description of this long-range order. That is why the explanation of the observed effect as the ac Josephson effect is by far the most convincing.

FUTURE OUTLOOK

We have been able to observe and identify, with convincing clarity, the ac Josephson effect in superfluid He. This provides strong support to the concepts fundamental to the description of superfluidity, viz., complex order parameter and the Josephson equation. A unified description of the behavior of superconductors and liquid He is thus put on a firm footing.

The phase slippage, a concept associated with the Josephson equation, is interpreted in terms of the motion of quantized vortices. We have made only a conjecture as to their generation and motion. For the understanding of the mechanism of phase synchronization, it would be worthwhile to study these vortices (vortex rings and/or lines) by an independent technique.

Another possible way of obtaining phase synchronization would be the use of second sound, rather than first sound, in the immediate vicinity of the orifice.

In the Josephson equation $\nu = \Delta\mu/h$ the chemical potential difference can be achieved in a variety of ways, e.g., by setting up (i) gravitational head difference, (ii) temperature difference, (iii) He^3 – He^4, composition difference, (iv) difference in the velocity of the fluid, etc. A study of the Josephson effect using such other terms in the chemical potential would prove extremely useful in the device applications of this effect, in addition to providing a firmer foundation for the theoretical basis.

It is also possible to devise more complex experiments, analogs of elegant experiments done by Mercereau and his colleagues in the case of superconductors.

ACKNOWLEDGMENT

I have benefited throughout the course of this work from the guidance and encouragement of B. S. Chandrasekhar.

---

†Work supported by the U. S. Air Force Office of Scientific Research under AFOSR Grant No. 565-66.

*Present Address: Department of Physics and Astronomy, University of Rochester, Rochester, New York 14627.

[1]F. London, Superfluids (John Wiley & Sons, New York, 1950), Vol. I, Introduction.

[2]F. London, Nature 141, 643 (1938).

[3]O. Penrose and L. Onsager, Phys. Rev. 104, 576 (1956).

[4]W. L. McMillan, Phys. Rev. 138, A442 (1965).

[5]H. K. Onnes, Leiden Comm. 122b, (1911); 124c, (1911).

[6]J. Bardeen, L. N. Cooper, and J. R. Schrieffer, Phys. Rev. 108, 1175 (1957).

[7]L. N. Cooper, Phys. Rev. 104, 1189 (1956).

[8]P. W. Anderson, Rev. Mod. Phys. 38, 298 (1966).

[9]L. P. Gor'kov, Zh. Eksperim. i Teor. Fiz. 34, B5 (1958) [English transl.: Soviet Phys. – JETP 7, 505 (1958)].

[10]B. D. Josephson, Advan. Phys. 14, 419 (1965).

[11]I. K. Yanson *et al.*, Zh. Eksperim. i Teor. Fiz. 48, 976 (1965) [English transl.: Soviet Phys. – JETP 21, 650 (1965)]; D. N. Langenberg *et al.*, Phys. Rev. Letters 15, 294 (1965); I. Giaever, *ibid.* 15, 1904 (1965).

[12]S. Shapiro, Phys. Rev. Letters 11, 80 (1963).

[13]P. W. Anderson and A. H. Dayem, Phys. Rev. Letters 13, 195 (1964).

[14]P. L. Richards and P. W. Anderson, Phys. Rev. Letters 14, 540 (1965).

[15]B. M. Khorana and B. S. Chandrasekhar, Phys. Rev. Letters 18, 230 (1967), where preliminary results of this paper were reported.

[16]H. A. Boorse and J. G. Dash, Phys. Rev. 79, 734 (1950); 82, 851 (1951).

[17]C. Blake and C. E. Chase, Rev. Sci. Instr. 34, 948 (1963).

[18]E. J. Walker, Rev. Sci. Instr. 30, 834 (1959).

[19]R. P. Feynman, in Progress in Low Temperature

Physics, edited by C. J. Gorter (North-Holland Publishing Co., Amsterdam, 1955), Vol I, Chap. II.

[20]This uncertainty has now been reduced to 1%. See B. M. Khorana and D. H. Douglass, Jr., in Proceedings of the Eleventh International Conference on Low Temperature Physics, edited by J. F. Allen, D. M. Finlayson, and D. M. McCall (University of St. Andrews Printing Department, St. Andrews, Scotland, 1969).

[21]R. J. Donnelly, Phys. Rev. Letters 14, 939 (1965); W. Zimmerman, *ibid.* 14, 976 (1965); Appendix B in Ref. 9.

[22]L. D. Landau, J. Phys. USSR 5, 71 (1941).

PHYSICAL REVIEW VOLUME 185, NUMBER 1 5 SEPTEMBER 1969

Divergences and the Approach to Equilibrium in the Lorentz and the Wind-Tree Models

G. Gallavotti
The Rockefeller University, New York, 10021
(Received 12 March 1969)

We prove that for wide class of physically interesting initial states the time evolution of the wind particles's correlation functions can be described at any finite time by a convergent power series in the density of the tree particles, provided this density is small enough. We show that all the coefficients (except the lowest ones) of this power series contain terms diverging as $t \to +\infty$. Nevertheless, we prove that the radius of convergence does not shrink to zero as $t \to +\infty$ and that the divergent terms can be resummed into a cutoff, thereby constructing a new series for the correlation functions having each term bounded as $t \to +\infty$. Although divergence free, this series does not converge uniformly in time; however, it can be used to show that equilibrium cannot be reached if the tree-tree interaction allows overlapping and to study the limiting case of vanishing tree size but nonvanishing free path; in this last case we find an exact expression for the Green's functions showing that the approach to equilibrium is described by a diffusion process which rigorously verifies the Boltzmann equation.

1. INTRODUCTION

A class of models was introduced by Lorentz and Ehrenfest, to all of which we will briefly refer as "wind-tree" models,[1-3] in order to understand some of the basic difficulties of the kinetic theory of gases.

In these models there are two types of particles: The "wind" particles move through the space interacting only with the particles of the second kind (the "tree" particles) which, however, are not supposed to be affected in their motion by the "light" wind particles and so are supposed to be in internal equilibrium under the action of their mutual forces. Each model is completely described by the wind-tree potential and by the tree-tree potential.

In this paper we shall examine only the case in which the trees are, with respect to the wind, either hard spheres or equally oriented hard cubes which reflect the wind on their surface.

We show that, if at time $t = 0$ the wind particles are in a nonequilibrium state which can be visualized as a state in which the wind is in equilibrium at temperature β^{-1} and chemical potential μ outside a certain finite region (where it is not in equilibrium), then the time evolution of the wind is described by a set of correlation functions (Sec. 3) that are analytic in the density n of the trees around $n = 0$ at any finite t (Sec. 4). We give explicit expressions for the coefficients of the expansion of the wind correlation functions in powers of the tree density n and we show that these coefficients (except the lowest ones) are sums of terms diverging in the limit $t \to \infty$ (Sec. 4). We study how these divergences can be eliminated by a resummation and we prove that the difference between the equilibrium correlation functions and the time-dependent correlation functions is given by a series (which is no longer a power series in n) in which the moduli of each term are uniformly bounded in time as is their sum (Sec. 5). Then we discuss the approach to equilibrium and show how to use the resummed series to exclude the possibility of approach to equilibrium in case the mutual interaction between the trees allows overlapping (Sec. 6). In Sec. 7 we study, for a free-tree gas, the limit-

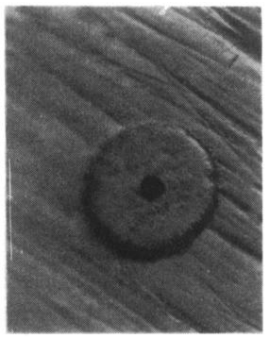

FIG. 2. Photograph of orifice in nickel foil.